Entrance Effects on Gas−Solid Riser Flow Structure

Jun You, Dawei Wang, and Chao Zhu*

Department of Mechanical Engineering, New Jersey Institute of Technology, Newark, New Jersey 07102

The gas−solid flow in a riser has strong inherent nonuniformities both in the flow structure and in the dynamic phases. The flow structure in a riser can be altered with the implementation of different solids feeding devices, and hence may affect the reactor performance. This paper is aimed at investigating the effect of various riser entrances on the overall flow structure and its stability at different operation conditions. Three riser entrances are selected to simulate the common solids feeding devices of risers, namely, the J-bend feeder, the L-valve feeder with a distributor, and the L-valve feeder after a taper section. The study is first focused on the flow dynamics in the riser entrance region. This is to identify the characteristic height of the entrance region as well as to obtain the radial distributions of phase transport properties at the end of the entrance region. These radial profiles are then used as the flow inlet conditions in the mechanistic model for the study of overall flow structure and stability in the riser main region. The study shows that the flow structure in the entrance region can be strongly affected by the selection of solids feeding patterns but weakly dependent upon the operation conditions. The flow structure in the main riser region, however, is weakly dependent upon the selection of solids feeding patterns but strongly affected by the operation conditions. The riser characteristic length of the entrance region is nearly independent of the gas inlet velocity and solids mass flow rate; however, it is moderately influenced by the solid feeding pattern. As part of model validation, some simulation results are directly compared with available experimental measurements, with reasonably good agreement.

1. Introduction

Gas−solid riser reactors, in which the solids are introduced into a vertical column from the bottom and transported by an upward gas flow against gravity, have been extensively used in various industrial applications, such as in coal gasification and petroleum refinery processes. The dense gas−solid riser flows have strong inherent nonuniformities in both the flow structure and the dynamic phases. The flow structure nonuniformity is typically in nonuniform distributions of phase velocities and concentrations within riser cross-sections as well as along the riser flow direction. The phase nonuniformity includes the nonuniform distributions among the dispersed solids, stable agglomerates, and transient clusters in the riser flow system. These inherent nonuniformities lead to many process concerns such as operation instability as well as nonuniform reactions or yields due to the nonuniformity in gas−solid contact and residence time, which hampers the continuous and high efficient operation of a riser reactor.

A thorough physical understanding and modeling interpretation of dynamic performance in a dense gas−solid riser reactor is a tremendously challenging task for researchers and engineers in the field. The axial heterogeneity in a general riser flow structure is mainly due to phase interactions including acceleration and dense-phase collisions, whereas the radial heterogeneity is mostly provided by the wall boundary effect.[1−8] The axial distribution of cross-section averaged transport properties such as solids concentration and solids velocity are empirically expressed in a "S-shape" form, with a dense-phase transport in the lower riser and a lean-phase transport in the upper part.[9] The radial distribution of solids concentrations in a cross-section away from the riser entrance region can be roughly described by a "core−annulus" structure or a "wall−annulus−core" structure, depending on the operation conditions.[10]

Mechanistically, the radial nonuniformity and even the flow instability are due to the wall boundary effect.[8] Due to turbulent diffusion in the core and damped gas flow near the wall, a dense layer of downward moving solids is informed in the wall region from the upper part of the riser, which is known as "backflow mixing". This downward moving layer of solids, coupled with re-entrainment of solids along its path, is mixed with upward-moving solids from the riser bottom, which results in a net radial-inward movement or entrainment of solids, as illustrated in Figure 1. As a result, the "core−annulus (wall)" flow structure, as shown in Figure 1A, often occurs at a low solids loading and/or at a high gas velocity, whereas the "core−annulus−wall" flow structure in Figure 1B can be formed at moderate solids loading and/or at a low gas velocity. With a high solids loading at low gas velocity, severe backflow mixing results in a local core of solids with a solid concentration peak, which not only causes the "core−annulus−wall" structure but also possibly triggers the flow instability or choking.

It is realized that although the characteristic height of the entrance zone is often only a small fraction of the total riser height, a significant portion of phase mixing and reaction may take place in the entrance region due to the relatively high solids holdup and long contact time. However, compared to the extensive understanding of the overall flow structure in a riser system (especially those in the dilute flow region), only a very limited knowledge has been gained for the riser entrance effect on the overall flow structure and riser flow stability. A recent experimental study[10] suggests that the overall flow structure and flow stability are only weakly affected by the variation in solids feeding methods, even though the entrance region and the flow mixing in that region can be strongly affected by the different feeding patterns or flow rates of solids. However, there is no available mechanistic model to explain such a claim and its generality, partly because of failure of 1-D flow approximation required by most of models and the failure of the uniform flow conditions assumed at the inlet of the modeling region.

This paper is aimed at investigating the effect of riser entrances on the overall flow structure and its stability at various solids feeding rates. Three riser entrances are selected to simulate

* To whom correspondence should be addressed. Tel.: 1 (973) 642-7624. E-mail: chao.zhu@njit.edu.

10.1021/ie8004868 CCC: $40.75
Published on Web 10/15/2008

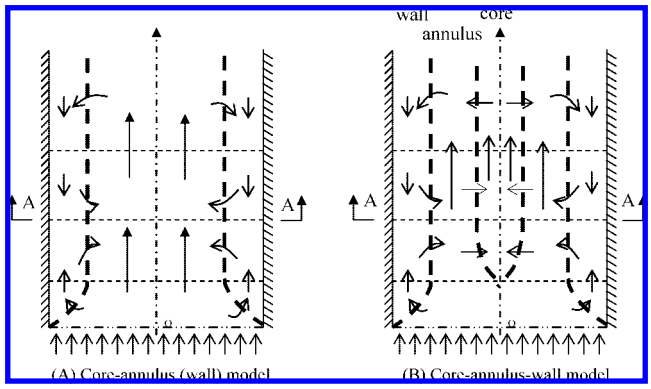

Figure 1. Heterogeneous flow structures in risers.

the common solids feeding devices of risers, namely, the J-bend feeder, the L-valve feeder with a fluidized bed distributor, and the L-valve feeder after an expansion section. The study is first focused on the flow dynamics in the riser entrance region. This is needed to identify the characteristic height of the entrance region (where the averaged gas−solid flow starts to be one-dimensional) as well as to obtain the averaged radial distribution of phase transport properties at the end of the entrance region. These radial profiles are then used as the flow inlet conditions in the 1-D mechanistic model for the study of overall flow structure and stability in the rest part of the riser. As a part of the model validation process, the simulation results are directly compared with available experimental measurements. For a generality study, the modeling is further applied to investigate some parametric effects of entrances over an extended operation regime. It can be concluded from the study that, at a similar solids loading and flow operation condition, the selection of various riser entrances indeed has a strong influence on the characteristic height, flow dynamics, and phase distributions within the entrance region but a weak impact on the flow structure and stability in the rest part of the riser. This finding is in general agreement with that indicated from the topographic measurements.[10]

2. Modeling Methodology

A riser flow can be conceptually divided into three regions, namely, the entrance region, the main region, and the exit region. In both the entrance and exit regions the flow is a multidimensional structure, whereas in the main region the flow can be approximated as one-dimensional. Due to the dominant effect of convection, the exit region is constantly assumed to have a weak impact on the flow structure in the main and entrance regions. Thus, for simplicity in the study of the entrance effect, the overall flow structure is considered only in the entrance and main regions, as shown in Figure 2.

Other key approximations in this study include the axial symmetry of the riser flow and the dispersed phase of solids (i.e., no clusters or agglomerates). These are introduced for the simplicity of mechanistic modeling and for the computer capacity limitation in the numerical simulation, especially with the consideration of gas−solid flows in the entrance region of a complex geometry. Thus, the flow in the entrance region is first investigated by means of a fine-grid 2-D numerical simulation approach, from which the characteristic length of the entrance region (at the end of which the flow becomes one-dimensional) can be defined and the radial distributions of phase transport properties (velocity and volume fractions) at the end the entrance region can be obtained. With these radial profiles

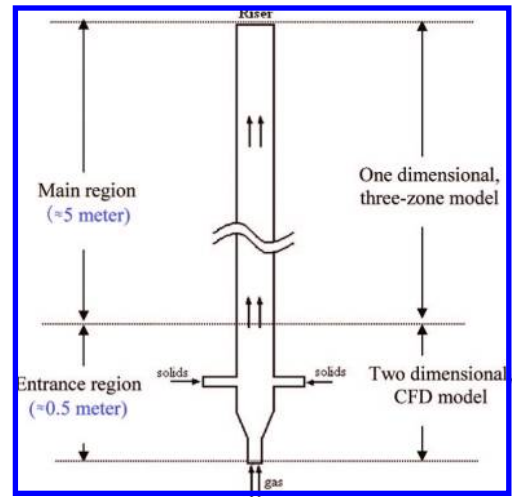

Figure 2. A two-region approximation for riser flow study of entrance effect.

Table 1. Quick Summary of 2-D and 3-D Simulation

		2-D	3-D coarse mesh	3-D fine mesh
equations need to solve	total	11	18	
	mass	1	1	1
	momentum	4	6	6
	$k-\epsilon$ model	2	2	2
	granular theory	4	5	5
total grid		6624	30185	761464
computation time		6 h[a]	51 h[a]	>1500 h[b]

[a] Computation time on a computer with 3.5 Ghz Pentium Dual-Core CPU and 3 GB memory. [b] Estimated calculation time.

as the flow inlet conditions, the flow structure in the rest part of the riser is then studied using a 1-D multizone mechanistic model, on which the flow stability can be further assessed.

Considering the complexity of dense gas−solid riser flow near the entrance region and the reality of availability of large computation capacity, 2-D approximation would be a good compromise for the present study though it may lose some 3-D characteristics of the entrance region. To provide a comprehensive physical model for gas−solids riser flows in the entrance region, one must consider the following mechanistic natures of the problem: (1) two phase flow, (2) turbulent flow, (3) interparticle collision dominated flow (granular flow theory), (4) multiscale size of feeding tube and riser, (5) complicated geometry (such as taped) riser entrances, (6) transient flow approach (for numerical solving stability).

A detailed comparison of computation capacities needed by 2-D and 3-D simulations is listed in Table 1. As a result, a 2-D approximation has to be adopted to accommodate all these requirements because of impractically long simulation time of 3-D simulation with a relatively reasonable grid amount. In order to provide a concrete comparison and check the rationality of 2-D simulation, one 3-D simulation based on fairly coarse mesh has been conducted and compared with 2-D simulation. Figure 3 presents the solids velocity and volume fraction profiles of the medium-plane of 3-D simulation and 2-D simulation. It could be observed that the two simulations bear certain similar patterns for both the velocity and volume fraction profiles. Hence, the 2-D simulation may provide similar characteristic descriptions of flow transport to that from 3-D simulation in the entrance region of gas−solid riser flows.

2.1. Selection of Typical Entrance Pattern. In order to examine the solids feeding pattern effects on the flow structure

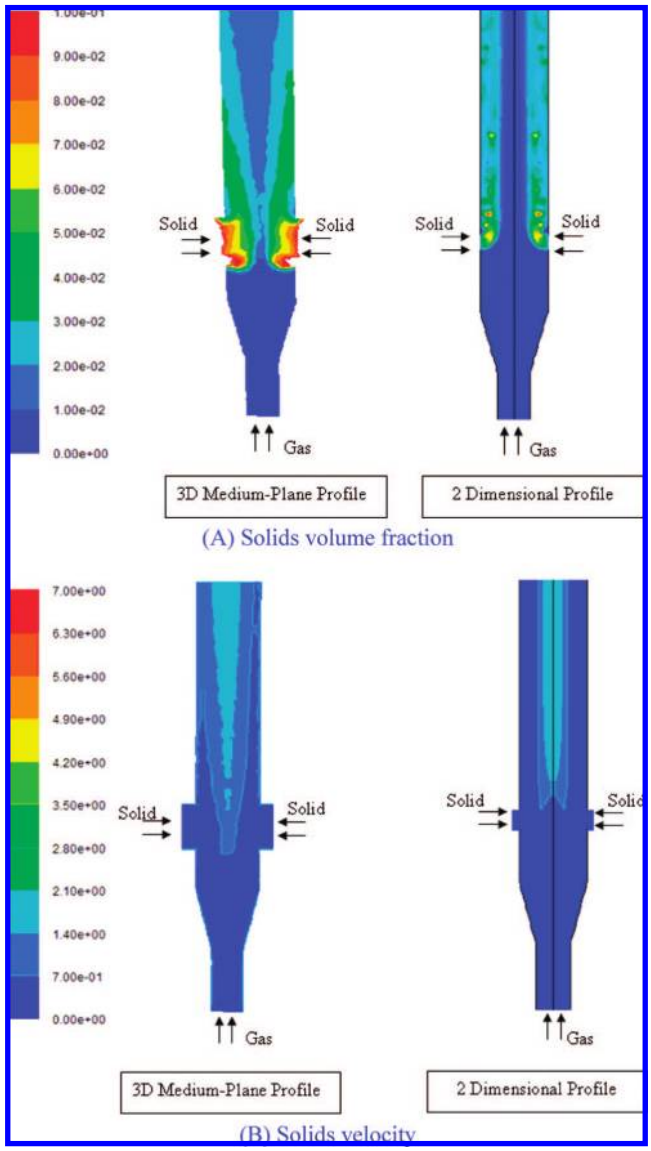

Figure 3. Comparison of 3-D vs 2-D simulation results in entrance region [U_g = 1.94 m/s, G_s = 11.9 kg/(m^2 s), 0.1 m i.d.].

and hydrodynamic characteristics of the riser, certain types of the entrance feeding patterns should be resolved to conduct the numerical simulation since in industrial facilities a wide variety of feeding patterns are adopted. Our selection concerns are mainly based on the availability of experimental validation and the representation of common solids feeding devices. Figure 4A illustrates some typical solids feeding patterns widely used in industrial applications and laboratory experiments, including (a) J-bend feeder, (b) L-valve feeder above a flow distributor, (c) L-valve feeder with an internal baffle, and (d) L-valve feeder after an expansion section. For the convenience of analysis and validation of our simulation without losing generality, three axial symmetric feeding patterns are selected, as shown in Figure 4B, representing (a) J-bend feeder or any feeders with a uniform solids flow at the bottom of riser, (b) annular ring of L-valve feeders above a flow distributor, and (3) annular ring of L-valve feeders after an expansion section.

2.2. Modeling of Gas−Solid Flow in Entrance Region. Gas−solid flow in the entrance region of a riser is not only multidimensional and multiphase but also transient in phase transport due to turbulence, phase instability (such as cluster formation and destruction), and interparticle collisions. Modeling of such a multiphase flow system is typically based on the volume−time averaging approach, described in either Lagrangian or Eulerian coordinates.[11] In this study, we adopt the Eulerian modeling for both gas and solids phases. For steady-state, nonreactive, and isothermal gas−solid flows, the general volume−time averaged equations can be expressed, respectively based on the mass and momentum conservation laws, as the following:

$$\nabla\cdot(\alpha_i\rho_i\mathbf{U}_i)=0 \quad i=\mathrm{s,g} \tag{1}$$

$$\nabla\cdot(\alpha_i\rho_i\mathbf{U}_i\mathbf{U}_i)=-\nabla p\delta_{ig}+\nabla\cdot\tau_i+\alpha_i\rho_i\mathbf{g}+\mathbf{F}_{Ai} \quad i=\mathrm{s,g} \tag{2}$$

In eq 2, $\mathbf{F}_A$ stands for the averaged interfacial momentum transfer or generalized drag force, $\boldsymbol{\tau}_g$ is the averaged shear stress of gas or turbulence stress, and $\boldsymbol{\tau}_s$ is the total solids stress due to interparticle collisions. In this modeling, the $k-\epsilon$ model is used to account for the turbulence effect, whereas the granular kinetic theory is used to account for the interparticle collision effect. As for the boundary conditions for the geometries in Figure 4B, the entrance region exit is set as outflow since the details of the flow velocity and pressure are not known prior to solution of the flow problem, and velocity inlet is set for the gas and solids inlets.

2.3. Modeling of Gas−Solid Flow in the Main Region. Volume−time averaged gas−solid flow in the main region of a riser can be approximated as steady and one-dimensional. However, due to the wall boundary effect, the radial distributions of phase transport properties are typically nonuniform, which nevertheless may be simplified by a three-zone representation, as illustrated in Figure 5. A schematic pattern of these three zones (namely, core, annulus, and wall zones) in the main region is shown in Figure 1B, with a uniform inlet flow condition. A mechanistic model to describe such a three-zone flow structure has already been developed by our research group.[8] In the current study of entrance effect, we apply this three-zone model to the cases with nonuniform inlet flow conditions predetermined from the modeling of entrance region. The length of the main region is estimated from the difference between the riser height and the characteristic length of entrance region (also determined from the modeling of entrance region).

On the basis of the core−annulus−wall flow structure with piecewise-uniform radial distributions, independent governing equations can be established, from mass and momentum conservations of each phase in each zone, as

$$G_gA=\sum_i\rho_g\alpha_{gi}U_{gi}A_i \quad i=\mathrm{a,c,w} \tag{3}$$

$$\frac{\mathrm{d}}{\mathrm{d}z}(\alpha_{si}\rho_sU_{si}A_i)=\dot{m}_{si} \quad i=\mathrm{a,c,w} \tag{4}$$

$$\frac{\mathrm{d}}{\mathrm{d}z}(\alpha_{gi}\rho_gU_{gi}^2A_i)=-\frac{\mathrm{d}p}{\mathrm{d}z}A_i-F_{Di}A_i-\alpha_{gi}\rho_ggA_i+\sum_{j\neq i}F_{fij} \quad i,j=\mathrm{a,c,w} \tag{5}$$

$$\frac{\mathrm{d}}{\mathrm{d}z}(\alpha_{si}\rho_sU_{si}^2A_i)=F_{Di}A_i-\alpha_{si}A_i\rho_sg+\frac{\mathrm{d}}{\mathrm{d}z}\left(C_{ppi}\frac{\mathrm{d}U_{si}}{\mathrm{d}z}\right)+\dot{M}_{si}+F_{fsi} \quad i=\mathrm{a,c,w} \tag{6}$$

3. Results and Discussion

In this section, the modeling results of flow structure are presented and discussed, in sequence, for the entrance effect in the entrance and main regions. First the simulations results are validated against the experimental results under comparable

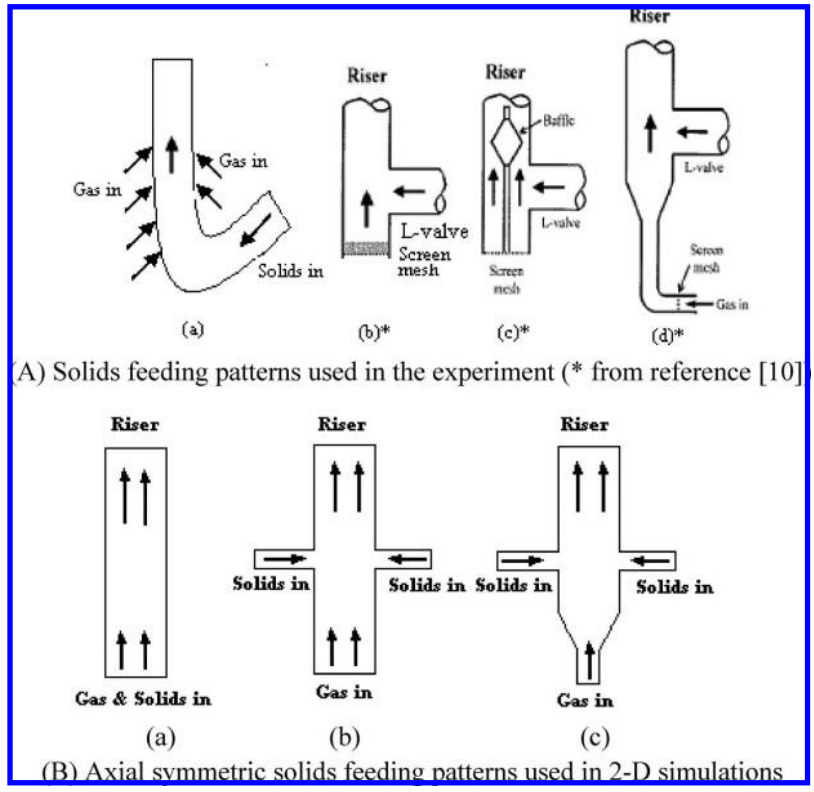

Figure 4. Selection of solids feeding patterns.

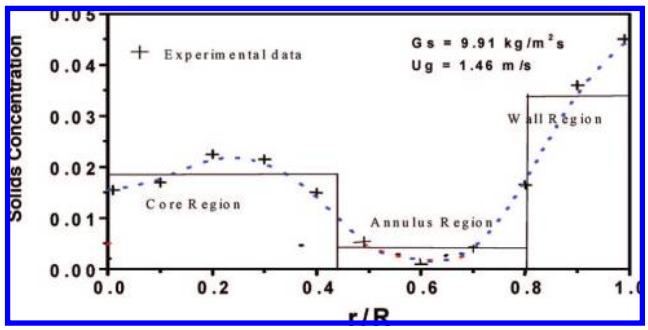

Figure 5. Three-zone representation of solids concentration distribution.[8]

entrance and flow conditions. Then a series of parametrical studies were performed to investigate the entrance effect on the characteristic length of the region and radial distributions of phase transport properties at the end of the entrance region, with various entrance and flow operation conditions. Finally, the flow structure in the main region and its variation at different entrance flow conditions are presented. Discussions are also extended to the parametric effects of entrance on the flow instability such as the possible occurrence of choking.

3.1. Flow Structure in Entrance Region. Numerical simulation of flow in the entrance region has been performed using the commercial code of FLUENT6.3. The geometry and mesh are generated using GAMBIT where the quad/triangle types of elements are used in the mesh generation process. In the basic setting of FLUENT, the axial-symmetric Eulerian multiphase model is selected. To capture the transient features of flow dynamics, the unsteady solver is adopted. The standard $k-\epsilon$ model is employed to describe the turbulence transport. In order to correctly predict the incipient or minimum fluidization conditions, the Syamlal−O'Brien empirical correlations for momentum transfer across the fluid−solid interfaces are introduced via a user-defined function. For the boundary conditions at the exit of entrance region, it is set as outflow since the details of the flow velocity and pressure are not known prior to solution of the flow. For the boundary conditions at the inlet of entrance region, uniform velocity profile is set for the gas, whereas the mass flow rate condition is given for the solids.

(A) Typical Flow Structure and Modeling Validation. Figure 6 illustrates the typical transient flow structure of phase transport properties in the entrance region, with the entrance of annular ring of L-valve feeders above a flow distributor that simulates case (a) as described by Du et al.[10] Figure 6A indicates that the transient spatial distribution of solids concentration may not be continuous, coupled with the formation and destruction of clusters. The transient flow structures in phase velocity however are relatively stable, as demonstrated in Figure 6B,C. A time-averaged flow structure can be obtained by averaging the transient results over a period of time that is longer than the integral characteristic time scale of the flow system.

It is realized that the published experimental data of phase distributions of transport properties in the entrance region are very scarce, which very much limits the validation of our simulation both in range and in accuracy. Figure 7 gives an example for the comparison of the time-averaged radial solids concentration distribution between the simulation results and the tomographic measurements from.[10] The riser inner diameter used in the experiment is 0.1 m, and the fluidized particles are FCC catalysts with a mean diameter of 60 μm and particle density of 1400 kg/m^3. The gas is fed from riser bottom, and solids are fed through the L-valve aeration on the side wall. The comparison indicates that the numerical simulation agrees reasonably well with the experimental measurements, which partially validates the simulation.

(B) Effect of Solids Feeding Patterns. For the convenience of investigating the effect of solids feeding patterns, the radial distributions of phase transport properties (i.e., solids concentration, solids velocity, and gas velocity) under various feeding

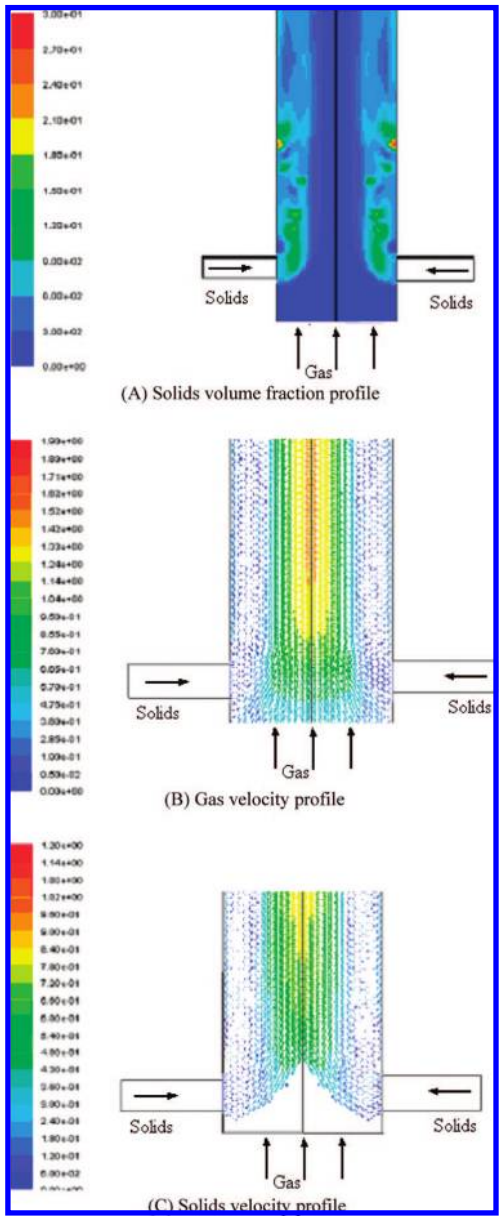

Figure 6. Transient flow structures in entrance region [U_g = 0.97 m/s, G_s = 1.32 kg/(m^{2}s), 0.1 m i.d.].

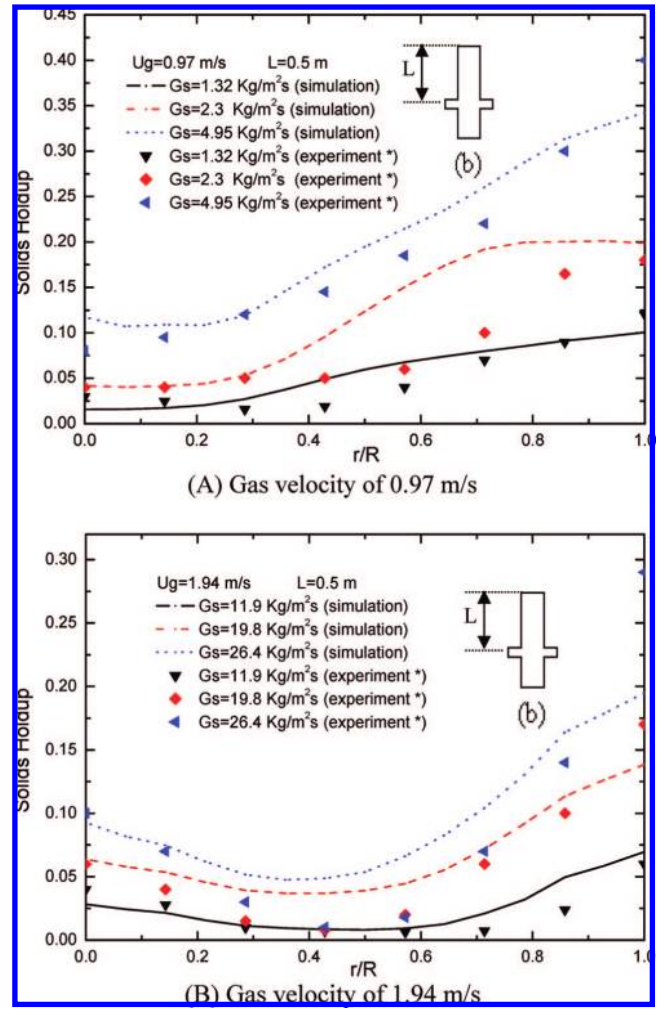

Figure 7. Radial distribution of solids concentration for simulation validation (* data are from reference 10).

patterns and operation conditions are compared in risers of the same diameter and at the same height above the level of solids entrance, as illustrated in Figures 8 and 9. Figure 8A shows that there exists a clear difference in solids concentration profiles with three different solids feeding patterns. For instance, the solids feeding type a leads to a very much even profile of solids concentration than those by other two types, whereas the cross-flow feedings may lead to sever solids accumulation near the wall. It is noticed that there is a moderate difference in all profiles between the feeding patterns b and c, which indicates a limited role of the taper section in the pattern c. Figure 8B shows much weaker gas velocities with the feeding patterns b and c near the wall, indicating a strong damp effect by the high solids concentrations near the wall. It is interesting to note that, as shown in Figure 8C, there is some backflow mixing with the feeding pattern c, whereas no backflow mixing occurs with other two feeding patterns at this level. This is probably due to the effect of taper section that weakens the gas flow near the wall, as shown in gas velocity profile in Figure 8B. Figure 9 shows the effect of solids feeding patterns on flow structures in the entrance regions, with an elevated solids mass flow rate and at an elevated gas velocity under otherwise similar operating conditions in Figure 8. Overall both Figures 8 and 9 present similar radial distribution profiles of phase transport properties, which indicates that the effect of solids feeding patterns in the entrance regions is strongly dependent upon the type of solids feeding mode (such as cross-flow feeding and concurrent flow feeding) but is weakly dependent upon the solids mass flow rate and gas velocity.

(C) Characteristic Length of Entrance Region. For a solids flow in the entrance region, a wall region of dense solids concentration has to be developed from the riser bottom because, due to the wall boundary effect, the averaged gas velocity in the wall region becomes too low to support upward moving solids. At a certain height, the solids in the wall region have to exhaust all their initial upward momentum against gravity as well as against the backflow mixing. At this location, the averaged solids velocity in the wall region is null, and beyond this characteristic height, solids in the wall region start to move downward (a phenomenon known as backflow mixing). The head-on impact of upward moving solids and backflow mixing solids is believed to be the major mechanism leading to the radial-inward moving migration of solids. The distance between the entrance location of solids feeding and this characteristic height (which is the turning point of the solid velocity) is defined in this paper as the characteristic length of entrance region. There is no well-established theory of determining the characteristic

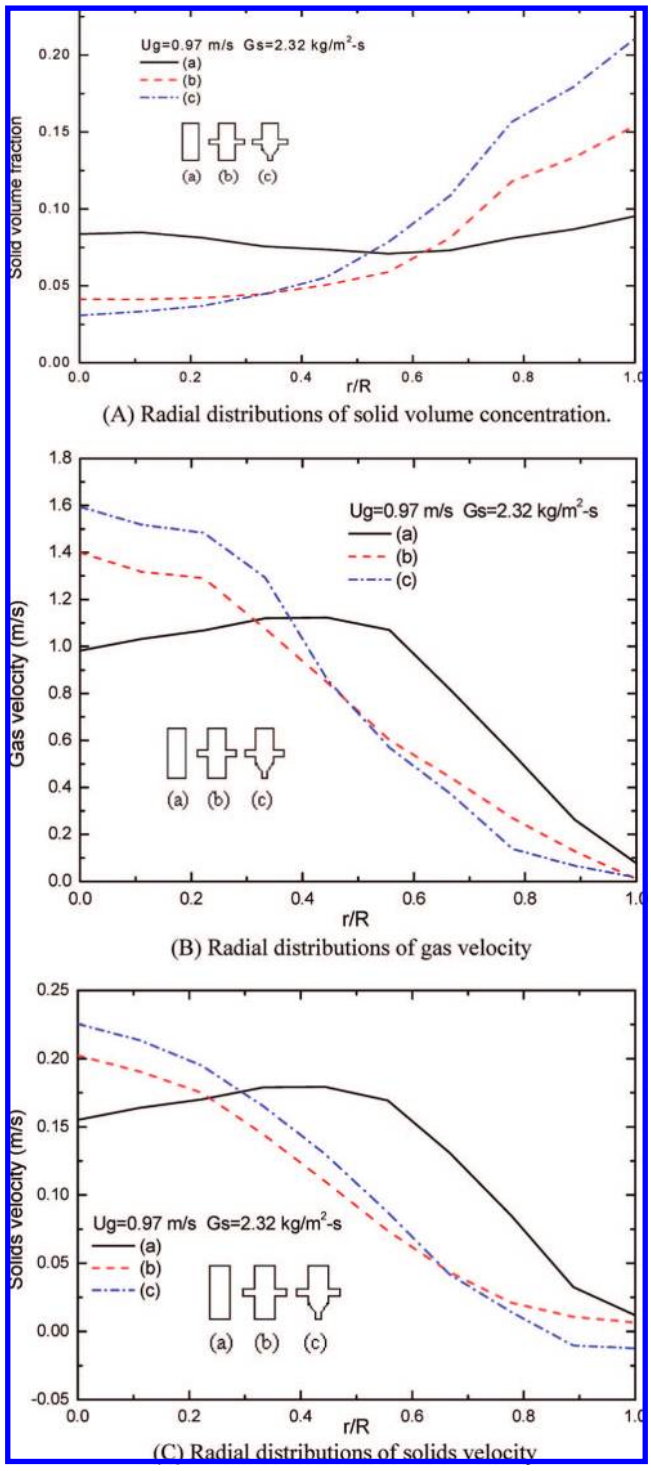

Figure 8. Effect of solids feeding patterns on radial profiles in entrance region (U_g=0.97m/s, G_s=2.32 kg/m^2-s, z=0.3 m).

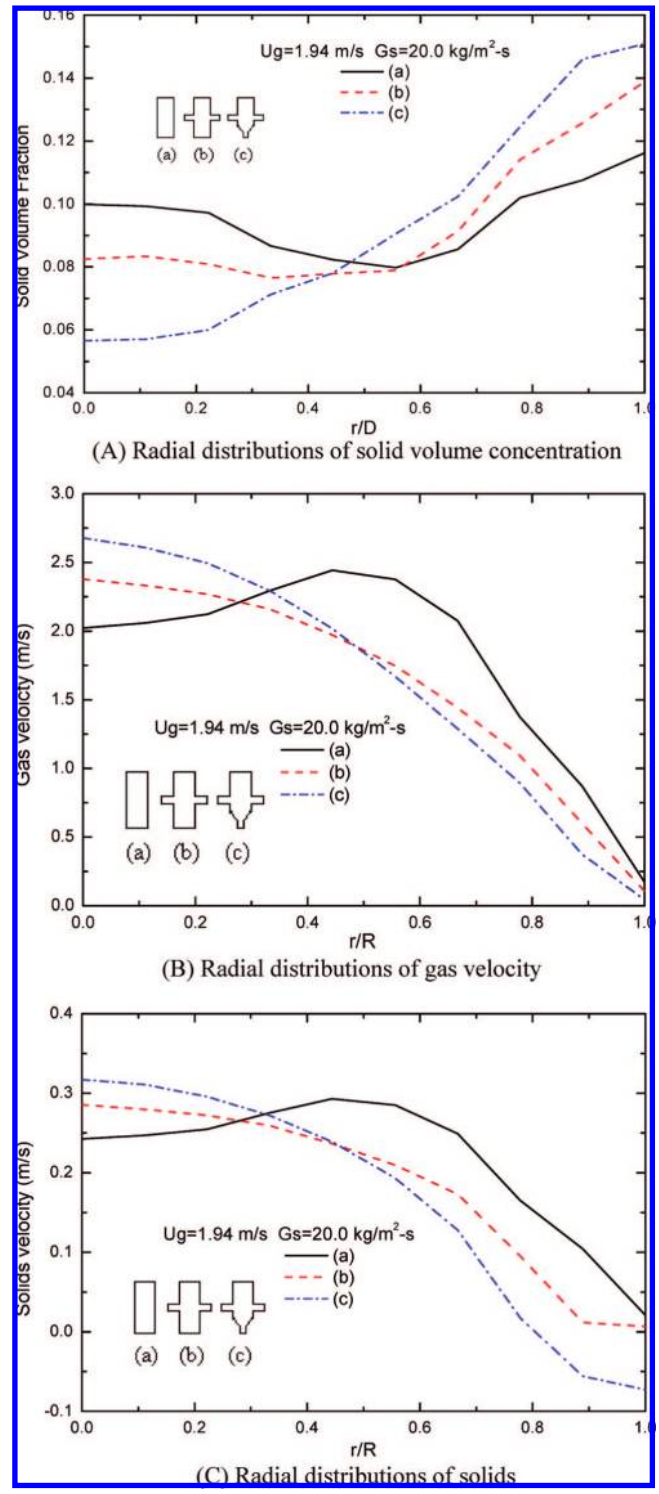

Figure 9. Effect of solids feeding patterns on radial profiles in entrance region (U_g = 1.94 m/s, G_s = 20.0 kg/(m^2 s), Z = 0.3 m).

length for the flow pattern transition from the multidimensional flow in the entrance to the approximated one-dimensional flow. In our paper, the characteristic length of entrance region is defined as the distance from the entrance of the riser to the point where the solid velocity at the wall decreases from entrance velocity to zero. Beyond this point, the flow pattern may be approximately characterized as one-dimensional. This definition is schematically illustrated in Figure 10. This characteristic length may also be used as a demarcation position for the flow pattern transition between the multidimensional flow in the entrance and one-dimensional flow approximation in the following main region of riser.

Figure 11 shows the effects of solids feeding patterns on this characteristic length of entrance region at various solids mass flow rates and gas velocities. It is noted that the characteristic length of entrance region is quite independent of solids mass flow rate and gas velocity; however, it is strongly dependent on the solids feeding pattern. After comparison, we can see that solids feeding type A has the largest characteristic length of entrance region, and the characteristic length of solids feeding pattern C is the smallest. Using a tracing technique, from the simulation, it can be observed that, starting from the solids entrance, solid moves upward with the very low initial axial

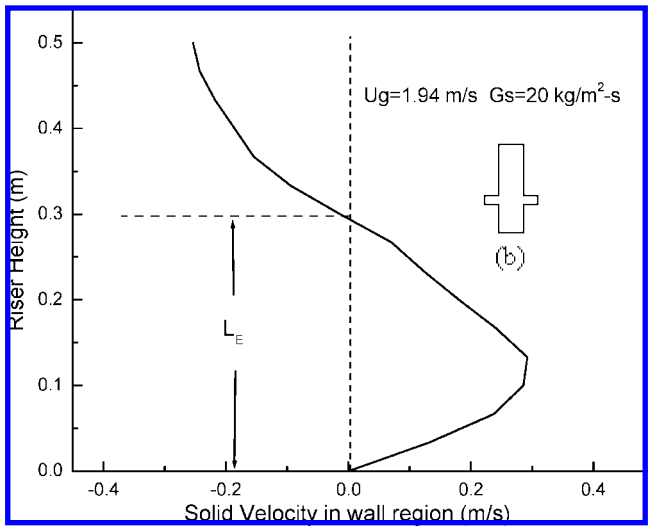

Figure 10. Definition of characteristic length of entrance region (L_E).

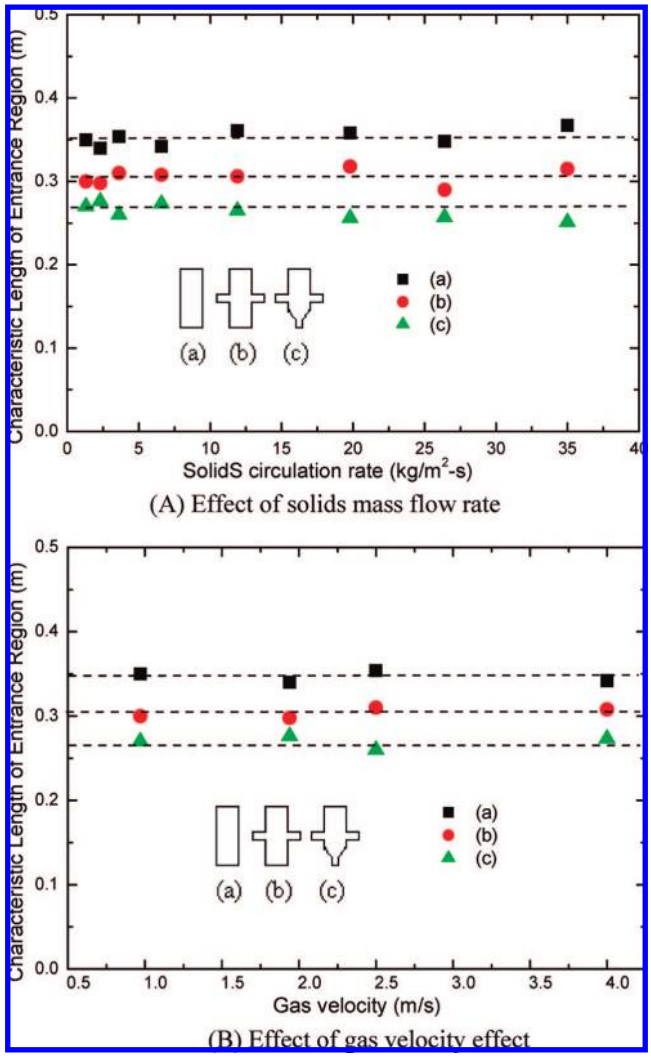

Figure 11. Effect of solids feed pattern on characteristic length of entrance region at various operation conditions.

velocity for all three cases. Once entering the riser, all solids, including those very close to the wall, experience a short period of acceleration and then quickly exhaust their inertia possibly by interparticle collisions. Beyond some certain height of riser, the solids near the wall begin to move downward. Figure 11A shows that the characteristic lengths of entrance region are 0.35, 0.31, and 0.26 m, respectively, for the three feeding patterns in this study.

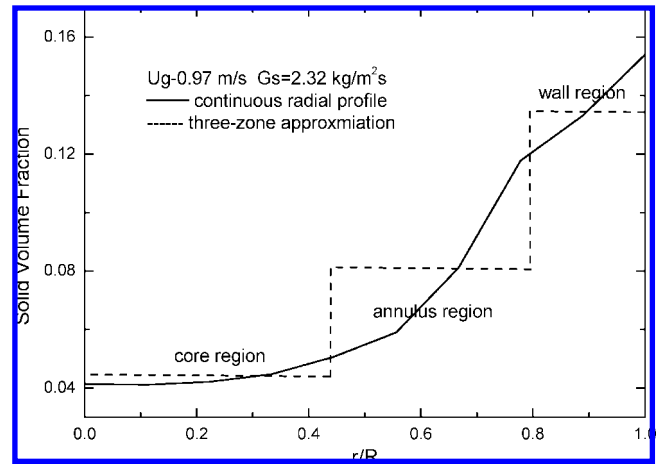

Figure 12. Three-zone approximation of inlet condition of solids concentration.

In the wall region of all three simulated solid feeding patterns, due to the solids−wall interactions and the nonslip of gas velocity at the wall, the drag force from the gas phase is insufficient to overcome the gravity and frictional forces of the solids; thus, solids near the wall will gradually lose their inertia and eventually their velocity will decrease to zero. So, the characteristic length of entrance region is basically decided by two factors: the solid initial momentum and averaged gas velocity in the wall region. Pattern A represents a configuration with a higher solids initial momentum and a relatively smaller slip velocity, which leads to a longer characteristic length of entrance region. Whereas pattern C has a relatively lower solids initial axial velocity and the smallest gas velocity in the wall region due to the expansion section of the riser, it has the smallest characteristic length of all three configurations considered.

3.2. Flow Structure in Main Region. As described in modeling methodology, the flow structure simulation in the main riser region is based on a modified mechanistic model originally developed by our research group.[8] Basic assumptions or requirements of this mechanics model include (1) one-dimensional flow; (2) three-zone flow structure, with predefined zone boundary or correlation; (3) neglect of interzone transport of gas phase; and (4) given radial distributions of phase transport properties at the inlet. The length of main riser region is the difference between the riser height and the characteristic length of entrance region.

(A) Three-Zone Approximation of Inlet Flow Conditions. On the basis of the flow structure simulation in the entrance region, the time-averaged radial distributions of phase transport properties at the end of the entrance region can be obtained, as exemplified in Figure 9. However, the mechanistic model of flow structure is currently based on a three-zone approximation, which calls for the zone-averaging over these continuous-based radial profiles, as exemplified in Figure 12. It should be pointed out that the selection of the three-zone boundary is not rigorously based on a scientific definition, but rather is based on the rough estimation from tomographic measurements of solids concentration.[8] The value of $r/R = 0.8$ for the wall region is our conservative estimate based on many reported radial distributions in velocity and solids concentration measurement in the dilute regime (although the extension into the dense regime near the riser entrance may be questionable), and $r/R = 0.45$ is our best estimate based on concentration transition from ECT

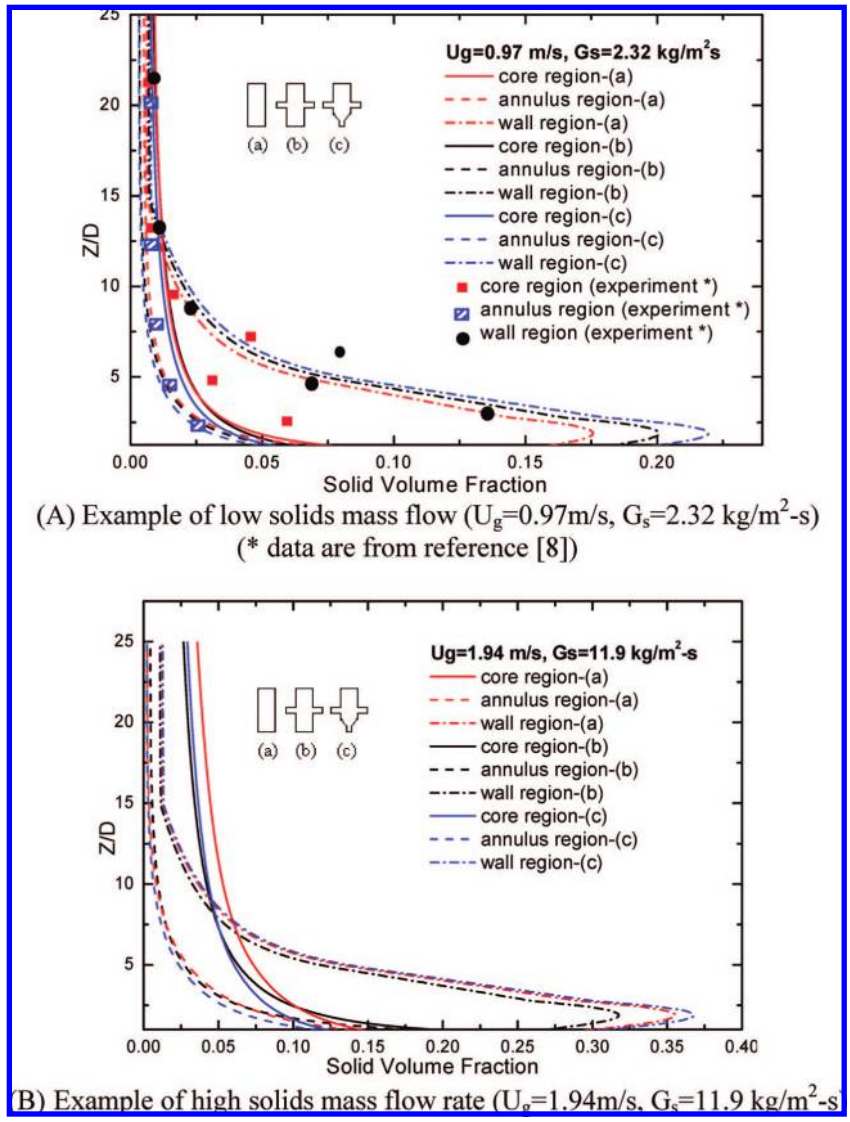

Figure 13. Effect of solids feeding patterns on axial distributions of solids concentration.

measurements. This approximation is in agreement with ECT findings. We understand these ratios could be dependent upon the riser flow characteristics such as riser size, transport regime, and overall flow conditions, which need to be considered in the future modeling.

(B) Effect of Entrance on Flow Structure. Figure 13 gives the effect of solids feeding pattern on the axial distributions of solid concentrations of each zone in the main riser region. It is shown that, at the same operation conditions, the use of different solids feeding patterns has no significant impact on the basic flow structures along the riser; namely, the axial distributions in each zone are weakly dependent on the type of solids feeding. Figure 13A shows that, with a low solids mass flow rate, there is little difference in solids concentration distributions between the core and annulus regions, indicating a two-zone flow structure. In the wall zone near the inlet of the main region, there exists a peak in the axial distribution of solids concentration. This may reflect the relatively delayed effect of solids acceleration near the wall as well as the strong coupling between the wall and annulus region. Beyond a certain height (say, $z/D > 10$), the axial distribution of solids concentrations becomes independent of the axial coordinate, indicating the fully developed state of flow structure. Figure 13B shows that, with a high solids mass flow rate, there is a clear three-zone flow structure throughout the entire main region. Similar to the case of low solids mass flow rate, beyond a certain height (in this case, $z/D > 15$), the flow reaches a fully developed state. In Figure 13A, the solids concentrations are also compared with the available experiment measurements in each region, and it shows a fairly good agreement.

Figure 14 demonstrated the effect of the solids feeding pattern on the axial distributions of solids velocity of each zone in the main riser region. A similar conclusion can be drawn from Figures 14A and 13B that different solids feeding patterns have no significant impact on the basic flow structure in the riser. In Figure 14A,B, it can be seen that, in the core region, there is an even smaller impact coming from the solids feeding patterns when compared with those impacts in the annulus and wall regions. It is interesting to notice that the solids velocity in the annulus region reaches its peak value at the height of $H/D = 15$ and then keeps this velocity through the rest of the riser, while in the core region, it is not true. The solids in the core region keep accelerating in the entirety of the riser, and its value is always lower than that in the annulus region. As for the solids in the wall region, it seems that there are no significant changes for the solids velocity and it always moves downward. Besides, in this wall region the impacts coming from solids feeding patterns are still very weak.

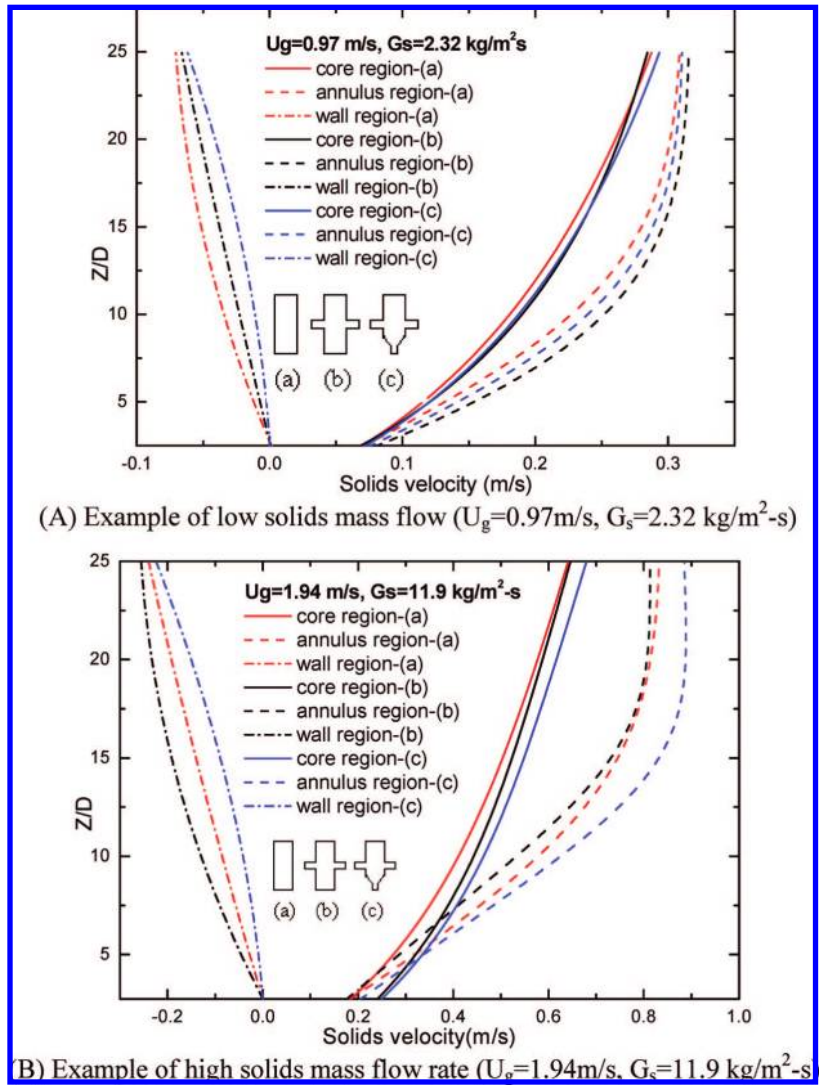

Figure 14. Effect of solids feeding patterns on axial distributions of solids velocity.

(C) Effect of Operation Conditions. So far, our simulation is limited to the operating conditions similar to those in the published experiment study in the literature.[10] It is interesting to speculate the effect of entrance on flow structure under other operation conditions, as illustrated in Figure 15 for the axial distribution of solids concentration. Figure 15A represents the case of low solids mass flow rate at a high gas velocity, whereas Figure 15B shows the typical case of high solids mass flow rate at a low gas velocity. Both cases suggest that the basic flow structure is weakly influenced by the type of solids feeding but strongly dependent on the operations conditions. With a significant increase in solids mass flow rate, as shown in Figure 15B, a reversal-hump-shaped distribution of solids concentration occurs in the core region. The initial decrease of solids concentration is due to the entrance effect on wall boundary layer development, whereas the hump results from a combined effect of a strong immigration of solids to the core region and a much reduced acceleration of the solids in the core region. The formation of the peak solids concentration in the core region can trigger the instability of the "core−annulus−wall" three-zone structure, as observed in the literature.[10] When the peak solids concentration is high enough, the flow-induced particle−particle interactions (such as wake-induced collisions) will lead to the collapse of the stable structure of solids in the core region, like choking, and hence the destruction of the entire flow structure in the riser.

4. Conclusion

This paper investigates the effect of various riser entrances on the overall flow structure and its stability at different operation conditions. Three riser entrances are selected to simulate the common solids feeding devices of risers, namely, the J-bend feeder, the L-valve feeder with a fluidized bed distributor, and the L-valve feeder after a taper section. For the purpose of validation, some simulation results are directly compared with available experimental measurements, and reasonably good agreements are reached. It was concluded that the riser characteristic length of entrance region is almost independent of gas inlet velocities and solids mass flow rates; however, it is moderately influenced by the solid feeding patterns. The study also shows that the flow structure in the entrance region can be strongly affected by the selection of solids feeding patterns but weakly dependent upon the operation conditions. According to the results of riser main region simulation, it is shown that, at the same operation conditions, the use of different solids feeding patterns has no significant impact on the basic flow structures along the riser; namely, the axial distributions in each zone are weakly dependent on the

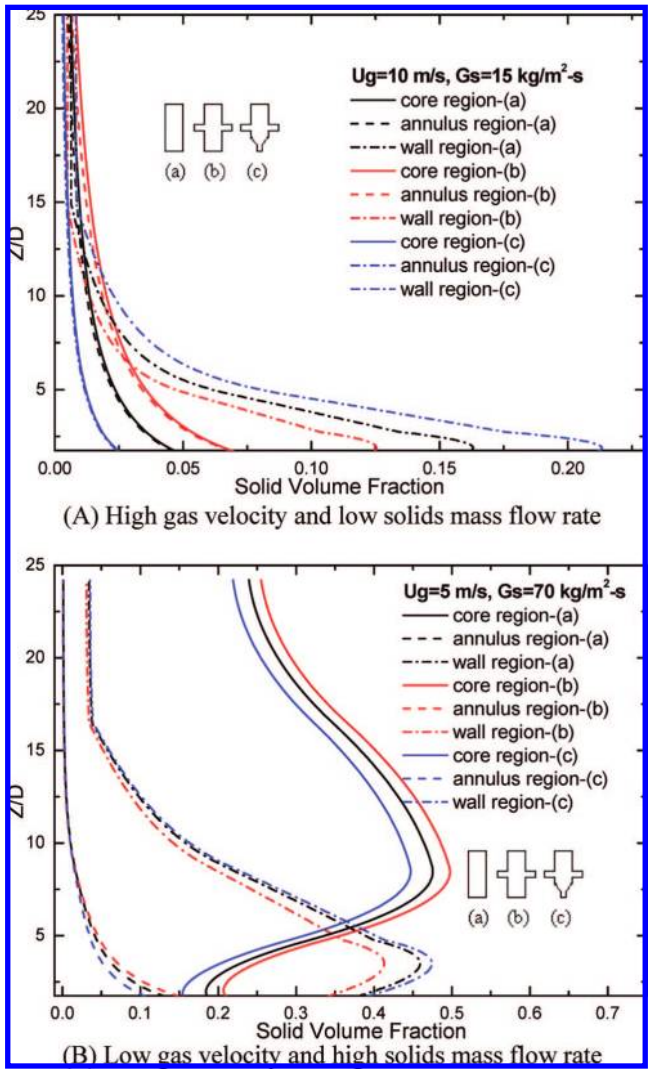

Figure 15. Parametric study of operation conditions on effect of entrance on flow structure.

type of solids feeding. Besides, it can also be concluded from the study that even the flow stability will not be significantly affected by the types of solids feeding patterns.

Acknowledgment

The authors would like to acknowledge the graduate assistantship from New Jersey Institute of Technology during the course of this study. The authors also would like to greatly acknowledge Professor L.S. Fan and Dr. Bing Du of Ohio State University for their helpful suggestions and for providing experimental data for the model validation.

Nomenclature

A_i = area
A_a = annulus regime area
C_{ppi} = transport coefficient
$\mathbf{F}_A$ = averaged interfacial momentum transfer or generalized drag force
F_{Di} = drag force
F_{fii} = friction force
g = gravity force
G = flow flux
m_s = net solids mass transfer of each zone
M_s = net solids momentum transfer of each zone
p = pressure
U = velocity
$\mathbf{U}$ = velocity vector of fluid
z = riser height
α = solid volume fraction
ρ = density
δ = Kronecker Delta
$\boldsymbol{\tau}$ = shear stress tensor

Subscripts

a = annulus region
c = core region
g = gas phase
s = solid phase
w = wall region

Literature Cited

(1) Louge, M.; Chang., H. Pressure and voidage gradients in vertical gas−solid risers. *Powder Technol.* **1990**, *60*, 197–201.

(2) Svensson, A.; Johnsson, F.; Leckner, B. Fluid-dynamics of the bottom bed of circulating fluidized bed boilers. In *Proceedings of the 12th International Conference on Fluidized Bed Combustion*; Rubow, L., Ed.; ASME: New York, 1993; pp 887−897.

(3) Horio, M.; Kuroki, H. Three-dimensional visualization of dilutely dispersed solids in bubbling and circulating fluidized beds. *Chem. Eng. Sci.* **1994**, *49* (15), 2413–2421.

(4) Sun, G.; Chao, Z.; Fan, Y.; Shi, M. Hydrodynamic behavior in the bottom region of a cold FCC riser. In *Circulating Fluidized Bed Technology VI*; Werther, J., Ed.; DECHEMA: Wurzburg, Germany, 1999; pp 179−184.

(5) Schlichthaerle, P.; Werther, J. Axial pressure profiles and solids concentration distributions in the CFB bottom zone. In *Circulating Fluidized Bed Technology VI*; Werther, J., Ed.; DECHEMA: Wurzburg, Germany, 1999; pp 185−190.

(6) Sabbaghan, H.; Gharebagh, R. S.; Mostoufi, N. Modeling the acceleration zone in the riser of circulating fluidized beds. *Powder Technol.* **2004**, *142*, 129–135.

(7) Zhu, C.; You, J. An energy-based model of gas−solids transport in a riser. *Powder Technol.* **2007**, *175*, 33–42.

(8) You, J.; Zhu, C.; Du, B.; Fan, L.-S. Heterogeneous structure in gas−solid riser flows. *AIChE J.* **2008**, *54* (6), 1459–1469.

(9) Li, Y.; Kwauk, M. The dynamics of fast fluidization. *Fluidization*; Grace. J. R., Matsen, J. M., Eds.; Plenum Press: New York, 1980; pp 537−544.

(10) Du, B.; Warsito, W.; Fan, L.-S. ECT studies of the choking phenomenon in a gas-solid circulating fluidized bed. *AIChE J.* **2004**, *50* (7), 1386–1406.

(11) Fan, L.-S.; Zhu, C. *Principle of Gas-Solid Flows*; Cambridge University Press: Cambridge, U.K., 1998.

Received for review March 27, 2008
Revised manuscript received July 21, 2008
Accepted August 28, 2008

IE8004868